JBC RESEARCH ARTICLE

Structural basis for the recognition of methylated histone H3 by the *Arabidopsis* LHP1 chromodomain

Received for publication, November 18, 2021, and in revised form, January 14, 2022 Published, Papers in Press, January 21, 2022,
https://doi.org/10.1016/j.jbc.2022.101623

Yanli Liu[1,*], Xiajie Yang[2], Mengqi Zhou[2], Yinxue Yang[1], Fangzhou Li[2], Xuemei Yan[1], Mengmeng Zhang[1], Zhengguo Wei[3], Su Qin[4], and Jinrong Min[2,*]

From the [1]College of Pharmaceutical Sciences, Soochow University, Suzhou, Jiangsu, PR China; [2]Hubei Key Laboratory of Genetic Regulation and Integrative Biology, School of Life Sciences, Central China Normal University, Wuhan, Hubei, PR China; [3]School of Biology and Basic Medical Science, Soochow University, Suzhou, Jiangsu, PR China; [4]Life Science Research Center, Southern University of Science and Technology, Shenzhen, Guangdong, PR China

Edited by Joseph Jez

Arabidopsis **LHP1 (LIKE HETEROCHROMATIN PROTEIN 1), a unique homolog of HP1 in *Drosophila*, plays important roles in plant development, growth, and architecture. In contrast to specific binding of the HP1 chromodomain to methylated H3K9 histone tails, the chromodomain of LHP1 has been shown to bind to both methylated H3K9 and H3K27 histone tails, and LHP1 carries out its function mainly via its interaction with these two epigenetic marks. However, the molecular mechanism for the recognition of methylated histone H3K9/27 by the LHP1 chromodomain is still unknown. In this study, we characterized the binding ability of LHP1 to histone H3K9 and H3K27 peptides and found that the chromodomain of LHP1 binds to histone H3K9me2/3 and H3K27me2/3 peptides with comparable affinities, although it exhibited no binding or weak binding to unmodified or monomethylated H3K9/K27 peptides. Our crystal structures of the LHP1 chromodomain in peptide-free and peptide-bound forms coupled with mutagenesis studies reveal that the chromodomain of LHP1 bears a slightly different chromodomain architecture and recognizes methylated H3K9 and H3K27 peptides via a hydrophobic clasp, similar to the chromodomains of human Polycomb proteins, which could not be explained only based on primary structure analysis. Our binding and structural studies of the LHP1 chromodomain illuminate a conserved ligand interaction mode between chromodomains of both animals and plants, and shed light on further functional study of the LHP1 protein.**

LIKE HETEROCHROMATIN PROTEIN 1 (LHP1), also known as TFL2 and TU8, was originally isolated from *Arabidopsis thaliana* independently by the screening of altered leaf glucosinolate levels mutants (1), of early flowering mutants (2), or of enhancers of the *terminal flower 1* mutants (3). LHP1 was then cloned independently by different groups using different methods (4–6). The allelic mutations of LHP1 show pleiotropic phenotypes, such as small plant size, curled leaves, terminal flowers, early flowering, reduced fertility, low glucosinolate content, and low roots growth rate (1–6), which indicate that LHP1 plays important roles in plant development, growth, and architecture.

Sequence analyses indicate that LHP1 is a homolog of *Drosophila* HP1 (heterochromatin protein 1) (7) and consists of an N-terminal chromodomain and a C-terminal chromo shadow domain, connected by a very long hinge region (4, 5, 8, 9). Further studies demonstrate that LHP1 is a unique homolog of *Drosophila* HP1 in the whole *Arabidopsis* genome (4, 5). HP1 is a critical nonhistone chromosomal protein, which is highly conserved from fission yeast to animals and plants and involved in heterochromatin formation and maintenance (10–12). It is well known that the chromodomains of HP1 proteins recognize methylated histone H3K9 (13–15), their chromo shadow domains mediate dimerization of HP1 proteins to form binding surface for the PxVxL motif or the PxVxL motif like-containing proteins (16, 17), and their hinge regions interact with DNA or RNA (18, 19). Hence, all the three parts of HP1 coordinate to play roles in chromatin condensation (13, 14, 18, 20). Similar to HP1 proteins in animals, the chromo shadow domain of LHP1 forms dimerization (5) and interacts with other proteins (21, 22), and the hinge region of LHP1 also binds to RNA (23). However, the chromodomain of LHP1 behaves differently from the canonical HP1 proteins. Some studies show that the chromodomain of LHP1 binds to methylated histone H3K9 *in vitro* (24, 25) and LHP1 colocalizes with heterochromatin enriched with methylated histone H3K9 *in vivo* (25, 26), and mutations of the methylated H3K9 cage-forming residues disrupt the colocalization (25). Other studies demonstrate that LHP1 binds to trimethylated histone H3K9 (H3K9me3) and H3K27 (H3K27me3) with similar affinities *in vitro*, however, LHP1 specifically colocalizes with H3K27me3 in euchromatin *in vivo* (27, 28). These data suggest that LHP1 may function similar to the Polycomb (Pc) protein of the polycomb repressive complex 1 (PRC11) (29, 30). Taken together, LHP1 may be present in both heterochromatin (25, 26) and euchromatin (31, 32), similar to mammal HP1γ (33), and all the chromodomain, chromo shadow domain, and hinge region are essential for chromatin engagement of LHP1 (25, 31). This scenario is consistent

* For correspondence: Jinrong Min, minjinrong@ccnu.edu.cn; Yanli Liu, ylliu18@suda.edu.cn.

with previous studies, which show that the HP1/LHP1 proteins are highly mobile and transiently interact with their nuclear loci (25, 34–36). Because the *lhp1* mutants generally affect genes in euchromatin (4, 32), the function of LHP1 in heterochromatin needs to be further elucidated.

As multiple phenotypes shown by *lhp1* mutants, LHP1 plays diverse roles during plant growth and development. LHP1 participates in flowering process by repressing two central flowering regulators, *FT* (*FLOWERING LOCUS T*, an activator gene of flowering) (4, 28) and *FLC* (*FLOWERING LOCUS C*, a repressor gene of flowering) (37, 38), and other floral homeotic genes, such as *AP3* (*APETALA3*), *PI* (*PISTILLATA*), *AG* (*AGAMOUS*), and *SEP3* (*SEPALLATA3*) (4, 32). LHP1 maintains repressive transcription of *FT* via recognizing and interacting with H3K27me3 (28), whereas LHP1 keeps epigenetic silencing of *FLC* via maintaining dimethylation status of H3K9 (38) or binding to this biomarker (37) during vernalization and upon return to warm conditions. LHP1 interacts with transcription factors AS1 and AS2 (ASYMMETRIC LEAVES 1 and 2) to repress the target genes to regulate leaf architecture (39). Because LHP1 holds Pc-like functions, binding to methylated H3K27 and interacting with plant RING-finger proteins, LHP1 is taken as a component of the plant PRC1-like complex, catalyzing histone H2A ubiquitylation (40, 41). However, recent research shows that *lhp1* mutants increase H2A ubiquitylation levels but decrease H3K27me3 levels, suggesting that LHP1 functions as a member of PRC2 but not PRC1 (39). Indeed, several studies illustrate that LHP1 works as the extra sex combs counterpart of PRC2 in animals (H3K27me3 binding and self-recruiting PRC2) and interacts with PRC2 and participates in establishing, spreading, and maintaining trimethylation of histone H3K27 (42–45).

Taken together, LHP1 plays important roles in plant development, and the interaction between LHP1 chromodomain and methylated histone H3K9 or H3K27 is critical for LHP1's functions. To better understand the mechanism of this interaction, in this study, we conducted quantitative binding assays and structural analyses of the LHP1 chromodomain with histone H3K9/K27 peptides. Our isothermal titration calorimetry (ITC) binding assays indicated that the LHP1 chromodomain binds to dimethylated or trimethylated H3K9/K27 peptides with comparable affinities, whereas no binding or weak binding to unmodified or monomethylated H3K9/K27 peptides. Our crystal structural studies provide molecular insights into lack of the selective binding of LHP1 to histone H3K9/K27 peptides.

Results and discussion

Chromodomain of Arabidopsis *LHP1 binds to histone H3K9me2/3 and H3K27me2/3 peptides with comparable affinities*

The chromodomains of HP1 and Pc in *Drosophila* are highly conserved and specifically recognize two sequence-related repressive histone markers, H3K9me3 and H3K27me3, respectively (46). The chromodomains of HP1 homologs in human, namely CBX1/HP1β, CXB3/HP1γ, and CBX5/HP1α, discriminate H3K9me3 from H3K27me3 effectively, whereas most Pc homologs in human (CBX2, 4, 6, 7, 8) bind to both H3K9me3 and H3K27me3 (47). To determine the binding ability of the LHP1 chromodomain in *Arabidopsis*, we measured the binding affinities of recombinant LHP1 chromodomain for both H3K9me3 (residues 1–15, with K9 trimethylated) and H3K27me3 (residues 19–33, with K27 trimethylated) peptides by ITC assays. Our data show that the LHP1 chromodomain binds to these two peptides similarly (Fig. 1), consistent with previous florescence polarization binding data (27). We further analyzed the effect of methylation states on the interaction and found that the LHP1 chromodomain bears similar binding affinities to both dimethylated H3K9 and H3K27 peptides, but no binding or weak binding to unmethylated or monomethylated cognates (Fig. 1). These data indicate that the chromodomain of LHP1 behaves differently from the HP1 and Pc proteins in *Drosophila*, but is similar to human Pc proteins.

Structure of the apo-form chromodomain of Arabidopsis *LHP1 indicates an uncanonical chromodomain conformation*

To illustrate the molecular mechanism of the interaction between the LHP1 chromodomain and methylated H3K9/K27 peptides, we tried to crystalize LHP1 chromodomain with or without methylated H3K9/K27 peptides of different lengths and solved the peptide-free and H3K9me3 (residues 5–10) peptide-bound crystal structures (Table 1 and Figs. 2 and 3). As shown in Figure 2, the structure of the apo LHP1 chromodomain is similar to the structures of previously reported HP1 or Pc chromodomains (47, 48), containing three β strands and a 3_{10} helix between the second and the third β strands followed by an α helix. The three β strands form a twisted antiparallel β-sheet harboring three potential methyllysine-binding, cage-forming aromatic residues Y108, W129, and W132 at one end of the β-sheet (Fig. 2*A*). However, a careful examination of the structure uncovers that the rings of the three aromatic residues are not mutually orthogonal, with the side chain of Y108 being parallel with that of W132, intruding into the potential methyllysine-binding pocket and making the pocket too shallow to fit for the methylated lysine residue (Fig. 2, *A* and *B*). This structural character indicates that there should be a conformational adjustment for the LHP1 chromodomain to interact with the methylated histone peptides.

Comparison of the structure of the LHP1 chromodomain to those of the HP1/Pc chromodomains reveals one dramatical difference in LHP1, which has an extra-long C-terminal α-helix approximately perpendicular to the β-sheet of LHP1 and forms an L-shape architecture (Fig. 2, *C* and *D*). In the chromodomains of HP1 and Pc, the α-helix is much shorter and packed against the β-sheet to form a sphere shape (49, 50). This extra-long α-helix is reminiscent of the second PWWP

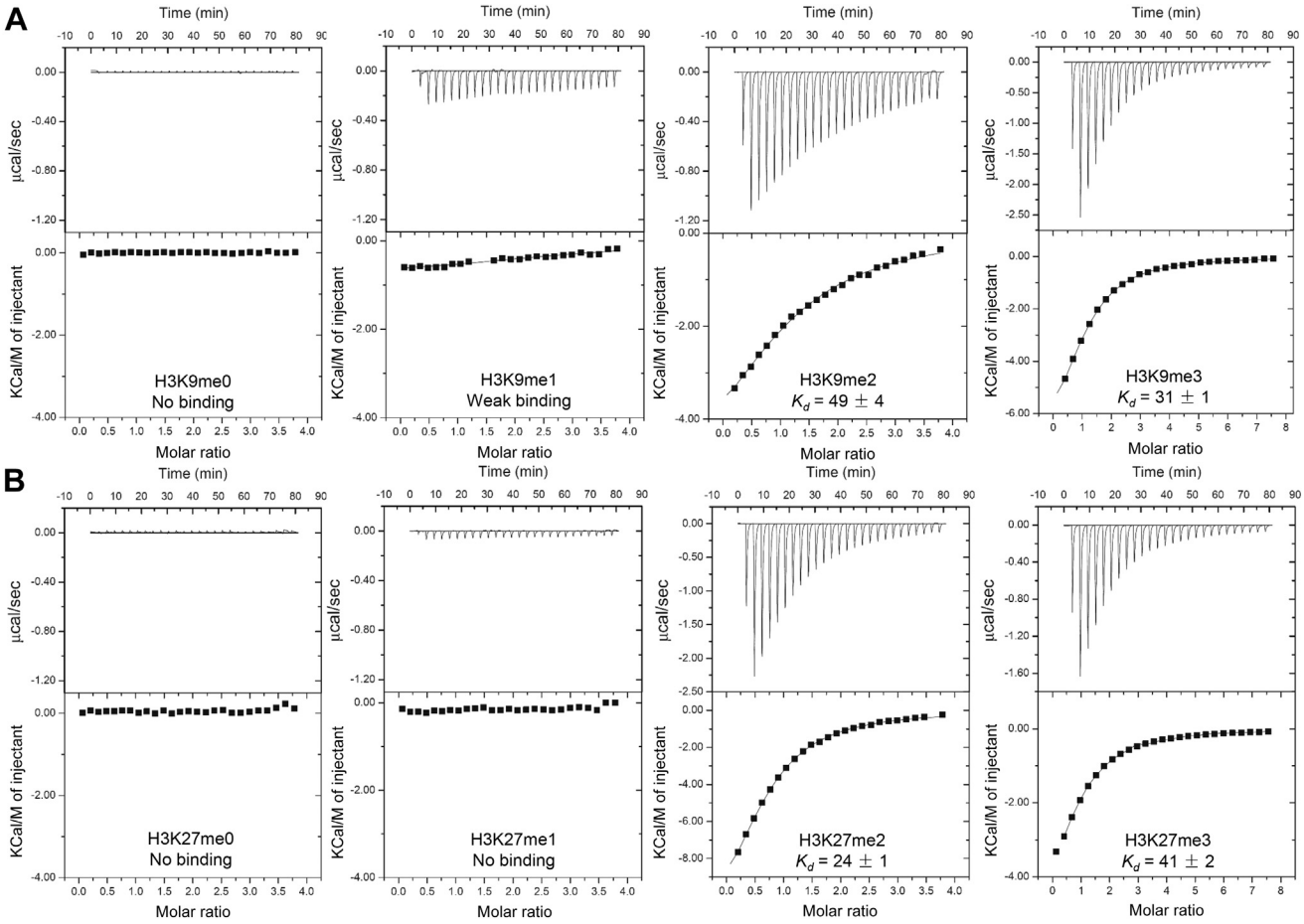

Figure 1. Chromodomain of *Arabidopsis* LHP1 protein binds to histone H3K9me2/3 and H3K27me2/3 peptides with similar affinities. Isothermal titration calorimetry binding curves of the chromodomain of LHP1 to H3K9me0-me3 peptides (*A*) and H3K27me0-me3 peptides (*B*), respectively. The data were obtained by VP-ITC microcalorimeter (MicroCal, Inc.).

domain (another member of Royal family) of NSD3, which also bears an extra-long α-helix; however, the PWWP's long helix shows a different orientation, packing against the β-sheet (51).

Taken together, our peptide-free structure dictates that the chromodomain of LHP1 is an uncanonical chromodomain and needs a conformational change for ligand binding.

Table 1
Data collection and refinement statistics

Parameter	LHP1	LHP1-H3K9me3
PDB code	7VZ2	7VYW
Data collection		
Space group	$P3_12_1$	$P2_12_12_1$
Cell dimensions		
a, *b*, *c* (Å)	31.7, 31.7, 106.4	26.1, 28.5, 70.5
α, β, γ (°)	90, 90, 120	90, 90, 90
Resolution (Å)	35.48–1.70 (1.73–1.70)	35.26 -1.60 (1.63 -1.60)
R_{merge}	0.035 (2.4)	0.035 (0.096)
R_{meas}	0.036 (2.458)	0.082 (0.166)
CC1/2	1.000 (0.87)	0.982 (0.968)
Mean (I/σI)	47.9 (2.1)	23.2 (6.4)
Completeness (%)	96.2 (93.4)	90.3 (81.9)
Redundancy	20.3 (20.8)	4.6 (2.7)
Model Refinement		
Resolution (Å)	35.48–1.70	35.26 -1.60
No. of reflections work/free	7088/721	6673/335
R_{work}/R_{free}	0.245/0.291	0.182/0.231
No. atoms/average B-factor [Å^2]	453/43.0	539/9.8
Protein	431/43.0	415/8.2
Peptide	n.a.	50/8.7
Water	17/43.1	59/19.0
RMSD bonds (Å)/angles (°)	0.006/0.8	0.007/1.05
Ramachandran plot residues in favored regions (%)	100.0	100.0

Values in parentheses are for the highest resolution shell.

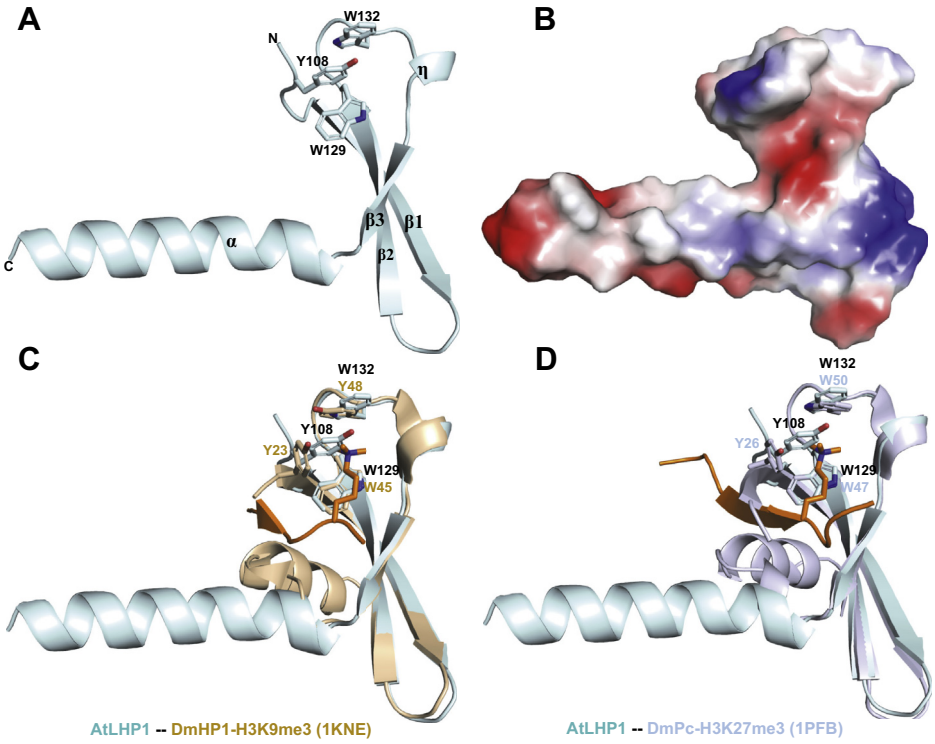

Figure 2. Structure of the apo-form chromodomain of *Arabidopsis* LHP1 indicates an uncanonical chromodomain conformation. *A* and *B,* the overall crystal structure of AtLHP1 chromodomain is shown as *cartoon* (*A*) or electrostatic potential surface representation (*B*), respectively. *C* and *D,* superposition of AtLHP1 on DmHP1-H3K9me3 complex (*C*) and DmPc-H3K27me3 complex (*D*), respectively. Structure figures were generated by using PyMOL. Electrostatic potential surface representations were calculated with PyMOL's built-in protein contact potential function (68).

Structural basis for selective binding of ARKme3S motif by the chromodomain of Arabidopsis *LHP1*

In the LHP1–H3K9me3 complex structure, the chromodomain of LHP1 undergoes tremendous conformational changes to accommodate the methyllysine of the H3K9me3 peptide, which will be discussed in details latter. Briefly, the N-terminal residues of the LHP1 chromodomain and the H3K9me3 peptide form two antiparallel β strands by using an induced-fit mechanism (Fig. 3*A*), which is also observed in the previous HP1-H3K9me3 complex structures (48, 49). The methylated K9 is surrounded by three cage-forming aromatic residues Y108, W129, and W132 to form cation-π interactions, similar to other methyllysine-binding domains (52–55), and several intermolecular hydrogen bonds between H3 peptide and LHP1 further stabilize the complex (Fig. 3, *B* and *C*). For example, H3Q5, H3A7, H3R8, and H3S10 form main-chain hydrogen bonds with I100, Y108, and N144 from LHP1, and H3R8 and H3S10 form side-chain hydrogen bonds with N144, S147, and E140, respectively (Fig. 3*B*). The aromatic cage-forming residues are essential for the ligand recognition and LHP1 stability, because the mutations of Y108 or W132 to alanine disrupt the binding, whereas the W129A mutant protein is insoluble (Fig. 3*D*). These cage-forming residues are also vital for the function of LHP1 *in vivo*, which has been confirmed by previous cage residue mutant studies (25, 56). In addition to the cation-π interaction, the side-chain hydrogen bonds between H3S10 and E140 are also indispensable, because the E140A mutation disrupts the peptide binding. This also suggests that the hydroxyl group of serine is important for the specific interaction and only serine or threonine can be tolerated at this site, consistent with the previous SPOT-blot assay (47). Furthermore, the interaction between the side chain of E140 and the hydroxyl group of serine/threonine are crucial for the chromodomain-ligand binding, because the glutamic acid residue is absolutely conserved in the chromodomains (Fig. 4*A*). On the other hand, the N144A mutant weakens, but does not abrogate binding. This also suggests that the arginine in the alanine-arginine-lysine-serine (ARKS) motif is replaceable, which is also in accordance with the previous SPOT-blot assay (47). Furthermore, all the mutants show similar binding behavior to both H3K9me3 and H3K27me3 peptides (Fig. 3*D*), indicating that the LHP1 chromodomain recognizes these two sites in a similar way.

In addition, the side chain of H3Q5 points away from the interaction surface, which indicates that the residue at this position is not critical for the specific interaction (Fig. 3*B*). H3T6 and the hydrophobic side chain but not the guanidino group of H3R8 are packed against two hydrophobic residues, F107 and A149, through hydrophobic interactions (Fig. 3*E*). Because the stabilization of H3T6 is mainly conferred by hydrophobic interactions, the corresponding residue H3A24 in the H3K27me3 peptide is also tolerated at this position. These two hydrophobic residues, namely F107 and A149, play an important role in binding to methylated H3K9 and H3K27 peptides, because the double mutations of these two residues to glycine significantly weakens the binding (Fig. 3*D*). H3A7 is anchored in a small hydrophobic pocket formed by residues

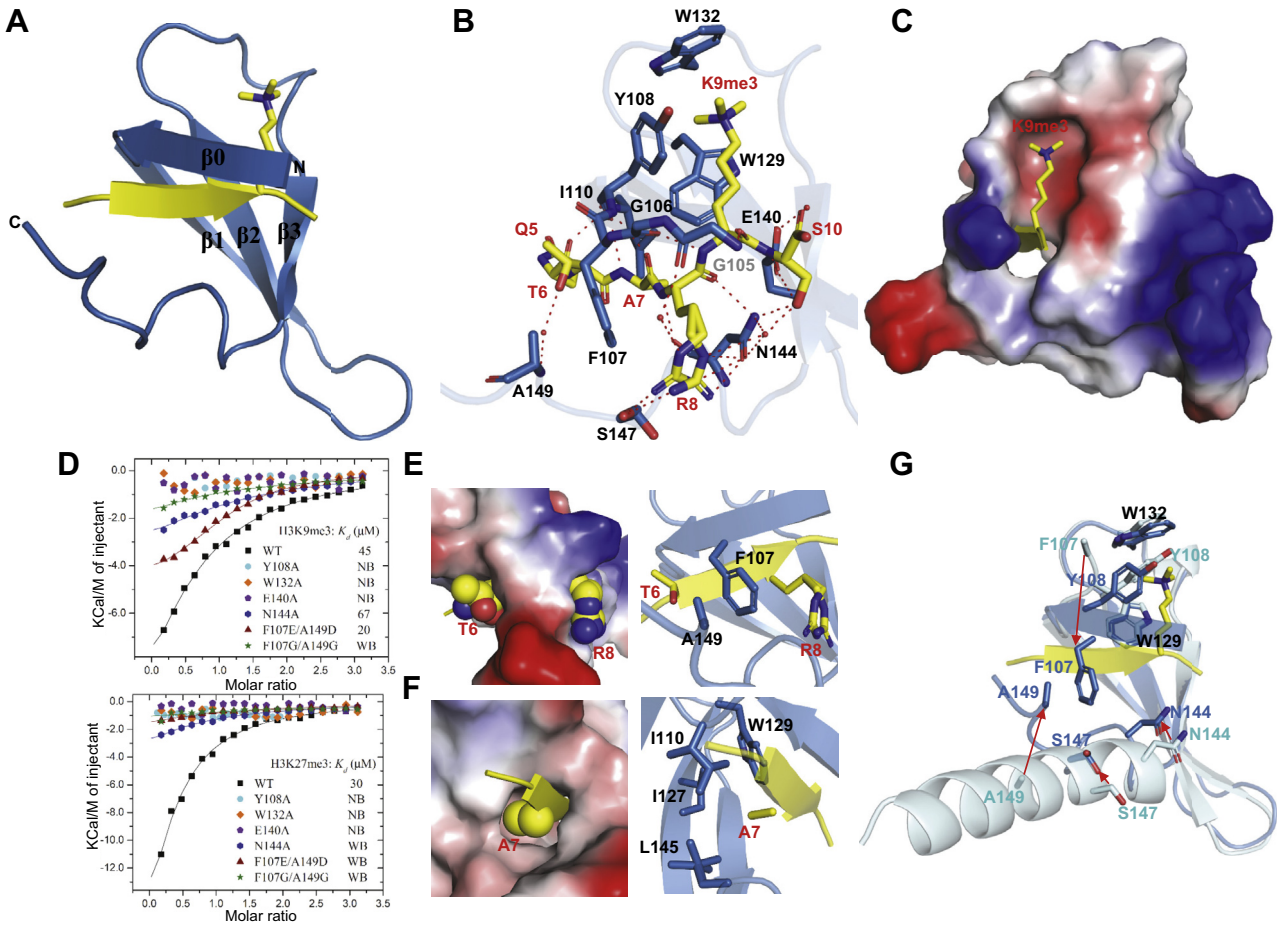

Figure 3. Structural basis for selective binding of histone H3K9/K27me3 peptide by chromodomain of *Arabidopsis* LHP1. *A,* overall structure of the chromodomain of LHP1 in complex with H3K9me3 peptide. The chromodomain and H3 peptide are shown in *cartoon* and colored in *blue* and *yellow*, respectively. *B,* detailed interactions of the histone H3K9me3 peptide with LHP1. The H3 peptide and H3-interacting LHP1 residues are shown in *stick* mode. Hydrogen bonds are shown as *red dashes*. *C,* the H3K9me3-binding pockets on the LHP1 chromodomain. *D,* mutation of the interacting residues affect the H3K9me3 and H3K27me3 binding. The data were obtained by iTC-200 microcalorimeter (MicroCal, Inc.). *E,* the hydrophobic residue pair for H3T6 and H3R8 recognition. *F,* the H3A7-binding pocket on the LHP1 chromodomain. *G,* superposition of LHP1-H3K9me3 complex on LHP1 peptide-free structure, with the cage-forming and significant conformation changed peptide-interacting residues are shown as *sticks*. NB, no detectable binding; WB, weak binding.

I110, I127, W129, and L145 and the side chain of alanine fits in the small hydrophobic pocket perfectly (Fig. 3*F*), which also determines the protein-ligand binding specificity. Taken together, our binding and complex structure analyses demonstrate that the methylated lysine at position 0 and alanine at position -2 of the ARKS motif are absolutely required, serine or threonine is tolerated at position +1, whereas replacement of arginine at position -1 by hydrophobic residues should be acceptable (Fig. 4*B*), which is consistent with previous Pc protein study (47). This also suggests that additional lysine-methylated protein ligands of LHP1 may remain to be discovered.

Comparison of peptide-free and peptide-bound LHP1 chromodomain structures uncovers two conformational changes: the disordered N-terminal to additional β strand and the C-terminal rigid long α helix to a flexible short loop (Fig. 3*G*). These conformational adjustments facilitate the protein-peptide interaction by forming methyllysine-binding cage for K9me3 and for the F107-A149 hydrophobic pair to hold H3T6, N144 and S147 moving close to the H3K9me3 peptide to enhance the interactions. Overall, our structural studies indicated that the chromodomain of LHP1 adopts several conformational changes to bind to the histone H3 peptide.

Comparison of the chromodomain of LHP1 to other chromodomains supports a conserved protein-ligand recognition mechanism

Structural and sequence comparison of the LHP1 chromodomain with other chromodomains indicated that the methyllysine cage-forming residues are highly conserved (Fig. 4*A*) and they bind to their ligands by similar binding modes (Fig. 5). In addition to the highly conserved cage-forming residues, the interacting residue for serine of ARKS, E140 in LHP1, is absolutely conserved too, which is consistent with its indispensable role in the interaction (Fig. 3*D*). Although the domain structures of LHP1 and HP1 are the same (4, 5, 8, 9), and their chromo shadow domains bind to similar motif-containing proteins (16, 17, 21, 22), our structure study

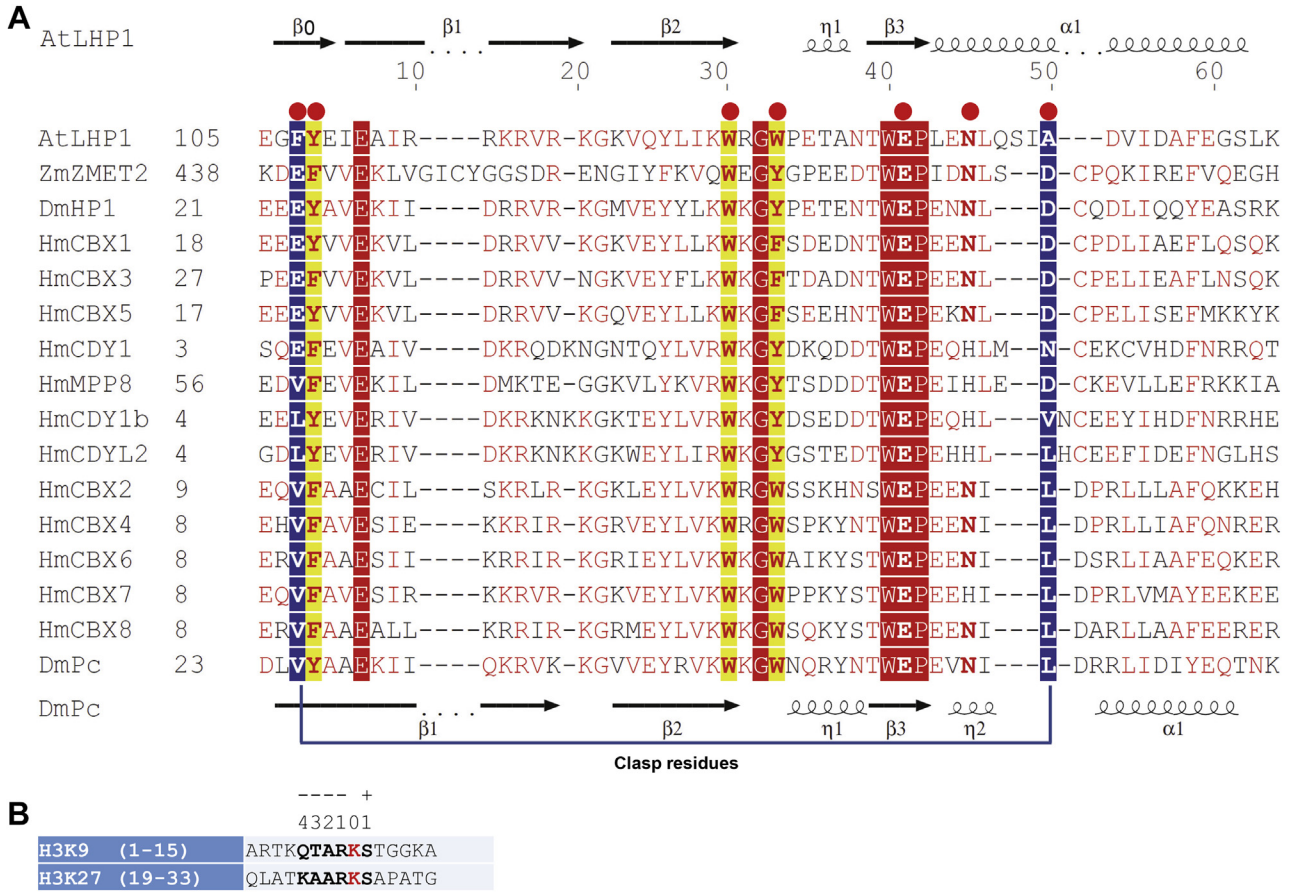

Figure 4. Structure-based sequence alignment of selective chromodomains. *A,* secondary structure elements of LHP1 and Polycomb group protein Pc of *Drosophila melanogaster* are indicated above or below the sequence alignment. The H3 peptide-interacting residues are marked by *red circles* with the cage-forming residues highlighted in *yellow* and clasp residues highlighted in *blue*. *B,* sequences of the H3K9 and H3K27 peptides used in this study, with the methylated lysine residue (*K*) highlighted in *red*. The residues in *bold* are for the short-length peptide. At, *Arabidopsis thaliana*; Zm, *Zea mays*; Dm, *Drosophila melanogaster*; Hm, *Homo sapiens*.

shows that their chromodomains bear different properties: the polar clasp in HP1 proteins decides their preference of binding to a methylated H3K9 histone tail, whereas the hydrophobic clasp in LHP1 and other human Pc proteins confers their binding to the two sequence-related methylated H3K9 and H3K27 histone tails more promiscuous (Figs. 4 and 5) (47, 57, 58). Our structural observation indicates that H3T6 is packed against a hydrophobic clasp formed by F107-A149, and H3T6-H3R8 also serves as a clasp to hold the "F107-A149 clasp" in turn (Fig. 3*E*), hence the hydrophobic clasp is important for the protein-ligand interaction in LHP1 as well (Fig. 3*D*). To explore if swapping the clasp residues of LHP1 with HP1 would change the binding selectivity of the LHP1 chromodomain, we made double mutations of the two clasp residues and found that the clasp residue swapping mutant does prefer to binding the H3K9me3 peptide over the H3K27me3 peptide (Fig. 3*D*), further validating the importance of the clasp residues in ligand selectivity of the LHP1 chromodomain. Based on the sequence alignment, Q146 of LHP1 is corresponding to the second residue of the "clasp residues" (Fig. 4*A*), which will not explain why LHP1 could bind to both H3K9me3 and H3K27me3 without structural information. Taken together, both our binding and structural studies indicate that LHP1 functions similar to human Pc proteins, and there may be other proteins resembling HP1 proteins in plants. Indeed, ADCP1 (Agenet Domain Containing Protein 1), a plant unique poly-Agenet domain (another member of Royal family in plant) containing protein has been verified as an HP1-like protein in plants (59).

The overall peptide-bound structures of LHP1 and other HP1/Pc homologs are similar, except the C-terminal conformational change to form an F107-A149 hydrophobic pair (Fig. 5, *A–E*). Structural comparison with another solved plant chromodomain, ZMET2 in *Zea mays*, suggests a similar ligand-binding induced C-terminal conformation change to form a polar clasp by E440 and D484 of ZMET2 to selectively bind to methylated H3K9 histone tail (Fig. 5*F*) (60). However, the C terminus of the ZMET2 chromodomain has the same orientation as the HP1/Pc chromodomains, which indicates that the new C-terminal direction of LHP1 chromodomain is a unique property.

In conclusion, our quantitative ITC-binding experiments illuminate that the chromodomain of LHP1 binds to dimethylated or trimethylated H3K9/K27 peptides without obvious sequence and methylation status preference, whereas it does not or weakly bind to unmethylated or monomethylated

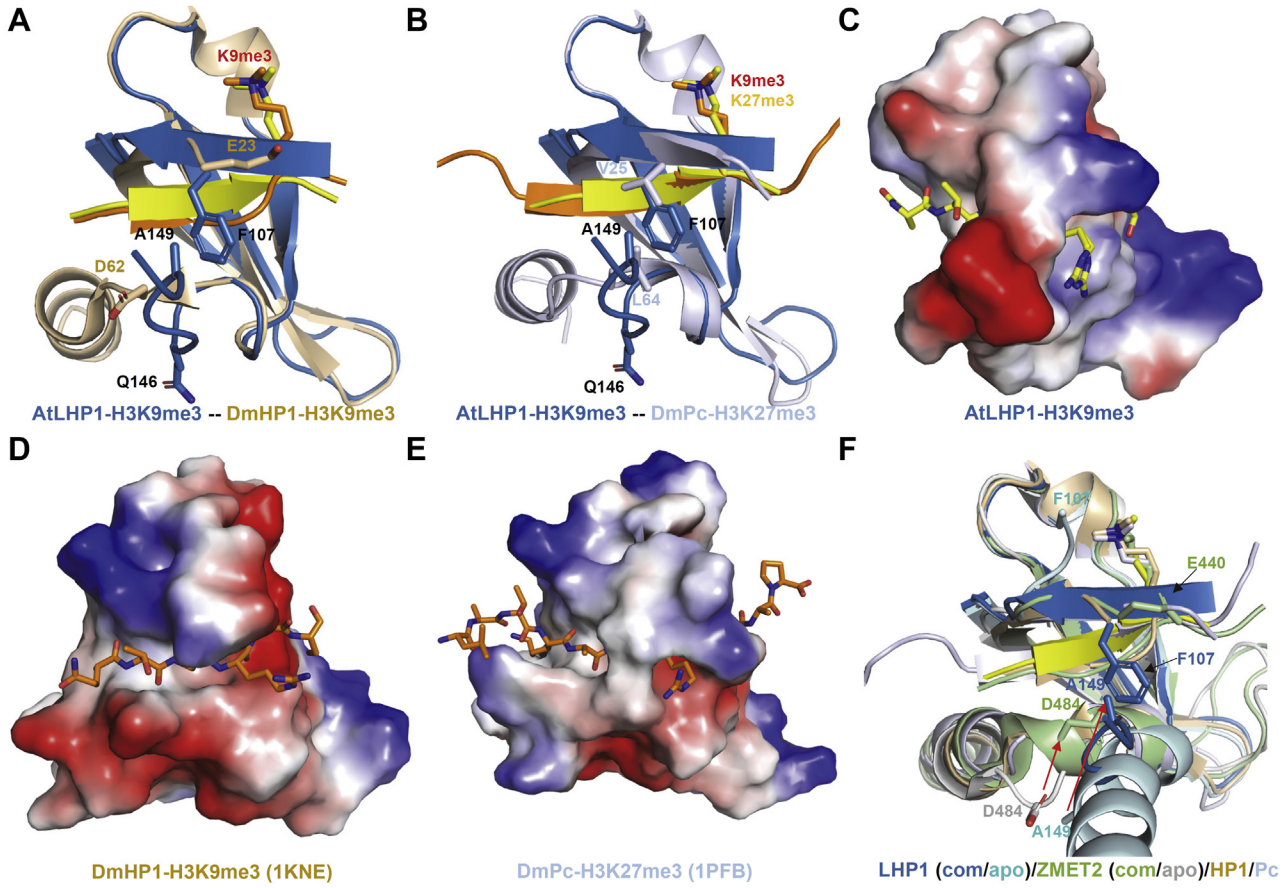

Figure 5. Structural comparison with other reported chromodomains. *A* and *B*, superposition of AtLHP1-H3K9me3 complex on DmHP1-H3K9me3 complex (*A*) and DmPc-H3K27me3 complex (*B*), respectively. *C–E*, electrostatic potential surface representation of AtLHP1 (*C*), DmHP1 (*D*), and DmPc (*E*) in the same orientation as (*A* and *B*), respectively. *F*, superimposition of AtLHP1-H3K9me3 complex on AtLHP1 peptide-free structure, ZmZET2-H3K9me3 complex, ZmZET2 peptide-free structure, DmHP1-H3K9me3 complex, and DmPc-H3K27me3 complex. The cage-forming and clasp residues are shown as *sticks* in figure *A*, *B*, and *F*.

cognates. Our structural analyses reveal that although LHP1 is a unique homolog of HP1 protein in plants, its chromodomain behaves similar to those of human Pc proteins and interacts with methylated H3K9/K27 histone tails by a hydrophobic clasp.

Experimental procedures

Protein expression and purification

The chromodomain of *Arabidopsis* LHP1 protein (residues 106–160) was subcloned into a modified pET28-MHL vector. The encoded N-terminally His-tagged fusion protein was overexpressed in *Escherichia coli* BL21 (DE3) Codon plus RIL (Stratagene) at 15 °C and purified by affinity chromatography on Ni-nitrilotriacetate resin (Qiagen, or Nanjing Qingning Bio-Technology Co., Ltd) followed by tobacco etch virus protease treatment to remove the tag. The tag-removed protein was purified by a second round of Ni-nitrilotriacetate resin to remove the His-tag and tobacco etch virus protease and then further purified by a Superdex75 gel-filtration column (GE Healthcare). The final purified protein was concentrated to 8∼30 mg/ml in a buffer containing 20 mM Tris–HCl, pH 7.5, 150 mM NaCl, and 1 mM DTT. The mutant constructs were generated by using QuickChange Site-Directed Mutagenesis Kit (Stratagene, 200,518), and all the mutant proteins were purified similar to the wild-type one. All the constructs used in this article were sequenced and confirmed.

Isothermal titration calorimetry

For the ITC measurement, the concentrated proteins were diluted into 20 mM Tris–HCl, pH 7.5, 150 mM NaCl; the lyophilized peptides for H3K9 (residues 1–15, with K9 at different methylation states) and H3K27 (residues 19–33, with K27 at different methylation states) (Wuhan Bioyeargene Biotechnology Co., Ltd or Shanghai Apeptide CO., Ltd) were dissolved in the same buffer, and the pH value was adjusted by adding NaOH. Peptides concentrations were estimated from the mass and the volume of the solvent. All the measurements were performed in duplicate at 25 °C, using a VP-ITC microcalorimeter (MicroCal, Inc.) or an iTC-200 microcalorimeter (MicroCal, Inc.). The protein with a concentration of 50 μM was placed in the cell chamber, and the peptides with a concentration of 0.75 to 2 mM in syringe was injected in 25 (20 for iTC-200) successive injections with a spacing of 180 s (150 s for iTC-200) and a reference power of 13 μcal/s (5 μcal/s for iTC-200). Control experiments were performed

under identical conditions to determine the heat signals that arise from injection of the peptides into the buffer. The data were fitted using the single-site binding model within the Origin software package (MicroCal, Inc.). iTC-200 data should be consistent with those from VP-ITC instrument, based on ITC results of same ITC assay using the two instruments.

Protein crystallization

For crystallization, the purified proteins were mixed with or without different length histone H3K9me3 or H3K27me3 peptides (encompassing residues 1–15, 19–33 as long form, and 5–10, 23–28 as short form), respectively. The mixture of protein and peptide with a molar ratio of 1:3 was crystallized using the sitting drop vapor diffusion method at 18 °C by mixing 0.5 μl of the protein with 0.5 μl of the reservoir solution. The peptide-free crystals were obtained in a buffer containing 20 mM Tris–HCl, pH 7.5, 150 mM NaCl, and 1 mM DTT. The complex crystals of chromodomain of LHP1 and histone H3K9me3 peptide (residues 5–10) were obtained in a buffer containing 0.1 M Hepes, pH 7.5, 2.0 M ammonium sulfate. Before flash-freezing crystals in liquid nitrogen, the crystals were soaked in a cryoprotectant consisting of 85% reservoir solution and 15% glycerol.

Data collection and structure determination

The diffraction data of peptide-free crystals and complex crystals were collected at a rotating copper anode x-ray generator and beamline BL17U1 of the Shanghai Synchrotron Radiation Facility (SSRF) at 100K, respectively. Diffraction images were processed using XDS (61)/POINTLESS/AIMLESS (62). PHASER (63) software was used for molecular replacement searches. COOT (64) was used for interactive model building. For the structure of peptide-free LHP1 was solved by molecular replacement with coordinates from PDB entry 1Q3L (deposited by Jacobs & Khorasanizadeh in 2003). After initial restrained model refinement with REFMAC (65), the model was automatically rebuilt with ARP/wARP (66). REFMAC and PHENIX (67) were used for further model refinement. The structure of LHP1–H3K9me3 complex was solved by molecular replacement with coordinates from the LHP1 crystal structure. REFMAC was used for restrained model refinement. Crystal diffraction data and refinement statistics for the structure were displayed in Table 1.

Data availability

Coordinates and structure factor amplitudes of LHP1 chromodomain and LHP1 chromodomain-H3K9me3 were deposited in the PDB with accession numbers 7VZ2 and 7VYW, respectively.

Acknowledgments—We would like to thank Dr Wolfram Tempel of University of Toronto, Zeyuan Guan of Huazhong Agricultural University, and Huan Zhou of SSRF beamline BL17U1 for assistance in data collection, Wolfram Tempel for structure determination, and Aiping Dong for reviewing the crystallographic models. We also thank the research associates at Center for Protein Research (CPR), Huazhong Agricultural University, for technical support. This work was carried out with the support of Shanghai Synchrotron Radiation Facility, beamline 17U1 (proposal 2019-SSRF-PT-010749). This work was supported by the National Natural Science Foundation of China grants (31500615), the Priority Academic Program Development of the Jiangsu Higher Education Institutes, China (PAPD), and Six-talent Professorship of Jiangsu province, China (SWYY-104).

Author contributions—Y. L. conceptualization; Y. L., X. Y., M. Z., Y. Y., F. L., X. Y., M. Z., Z. W., and S. Q. methodology; Y. L., X. Y., M. Z., Y. Y., F. L., X. Y., M. Z., and Z. W. investigation; Y. L., S. Q., and J. M. writing–original draft; Y. L., X. Y., M. Z., Y. Y., F. L., X. Y., M. Z., Z. W., S. Q., and J. M. writing–review and editing; Y. L., Y. Y., and J. M. visualization; Y. L. and J. M. supervision; Y. L. funding acquisition; Y. L., X. Y., M. Z., Y. Y., F. L., X. Y., M. Z., Z. W., S. Q., and J. M. formal analysis.

Conflict of interest—The authors declare that they have no conflicts of interest with the contents of this article.

Abbreviations—The abbreviations used are: ITC, isothermal titration calorimetry; LHP1, LIKE HETEROCHROMATIN PROTEIN 1; HP1, heterochromatin protein 1; Pc, Polycomb; PRC, polycomb repressive complex.

References

1. Haughn, G. W., Davin, L., Giblin, M., and Underhill, E. W. (1991) Biochemical genetics of plant secondary metabolites in Arabidopsis thaliana: The glucosinolates. *Plant Physiol.* **97**, 217–226
2. Bechtold, N., Ellis, J., and Pelletier, G. (1993) In-planta agrobacterium-mediated gene-transfer by infiltration of adult Arabidopsis-thaliana plants. *C. R. Acad. Sci.* **316**, 1194–1199
3. Larsson, A. S., Landberg, K., and Meeks-Wagner, D. R. (1998) The TERMINAL FLOWER2 (TFL2) gene controls the reproductive transition and meristem identity in Arabidopsis thaliana. *Genetics* **149**, 597–605
4. Kotake, T., Takada, S., Nakahigashi, K., Ohto, M., and Goto, K. (2003) Arabidopsis TERMINAL FLOWER 2 gene encodes a heterochromatin protein 1 homolog and represses both FLOWERING LOCUS T to regulate flowering time and several floral homeotic genes. *Plant Cell Physiol.* **44**, 555–564
5. Gaudin, V., Libault, M., Pouteau, S., Juul, T., Zhao, G. C., Lefebvre, D., and Grandjean, O. (2001) Mutations in LIKE HETEROCHROMATIN PROTEIN 1 affect flowering time and plant architecture in Arabidopsis. *Development* **128**, 4847–4858
6. Kim, J. H., Durrett, T. P., Last, R. L., and Jander, G. (2004) Characterization of the Arabidopsis TU8 glucosinolate mutation, an allele of TERMINAL FLOWER2. *Plant Mol. Biol.* **54**, 671–682
7. James, T. C., and Elgin, S. C. R. (1986) Identification of a nonhistone chromosomal protein associated with heterochromatin in Drosophila-melanogaster and its gene. *Mol. Cell. Biol.* **6**, 3862–3872
8. Paro, R., and Hogness, D. S. (1991) The Polycomb protein shares a homologous domain with a heterochromatin-associated protein of Drosophila. *Proc. Natl. Acad. Sci. U. S. A.* **88**, 263–267
9. Aasland, R., and Stewart, A. F. (1995) The chromo shadow domain, a second chromo domain in heterochromatin-binding protein 1, HP1. *Nucleic Acids Res.* **23**, 3168–3173
10. Li, Y. H., Kirschmann, D. A., and Wallrath, L. L. (2002) Does heterochromatin protein 1 always follow code? *Proc. Natl. Acad. Sci. U. S. A.* **99**, 16462–16469
11. Eissenberg, J. C., and Elgin, S. C. R. (2000) The HP1 protein family: Getting a grip on chromatin. *Curr. Opin. Genet. Dev.* **10**, 204–210
12. Maison, C., and Almouzni, G. (2004) HP1 and the dynamics of heterochromatin maintenance. *Nat. Rev. Mol. Cell Biol.* **5**, 296–304

13. Bannister, A. J., Zegerman, P., Partridge, J. F., Miska, E. A., Thomas, J. O., Allshire, R. C., and Kouzarides, T. (2001) Selective recognition of methylated lysine 9 on histone H3 by the HP1 chromo domain. *Nature* **410**, 120–124
14. Lachner, M., O'Carroll, N., Rea, S., Mechtler, K., and Jenuwein, T. (2001) Methylation of histone H3 lysine 9 creates a binding site for HP1 proteins. *Nature* **410**, 116–120
15. Nakayam, J., Rice, J. C., Strahl, B. D., Allis, C. D., and Grewal, S. I. S. (2001) Role of histone H3 lysine 9 methylation in epigenetic control of heterochromatin assembly. *Science* **292**, 110–113
16. Smothers, J. F., and Henikoff, S. (2000) The HP1 chromo shadow domain binds a consensus peptide pentamer. *Curr. Biol.* **10**, 27–30
17. Liu, Y., Qin, S., Lei, M., Tempel, W., Zhang, Y., Loppnau, P., Li, Y., and Min, J. (2017) Peptide recognition by heterochromatin protein 1 (HP1) chromoshadow domains revisited: Plasticity in the pseudosymmetric histone binding site of human HP1. *J. Biol. Chem.* **292**, 5655–5664
18. Muchardt, C., Guilleme, M., Seeler, J. S., Trouche, D., Dejean, A., and Yaniv, M. (2002) Coordinated methyl and RNA binding is required for heterochromatin localization of mammalian HP1 alpha. *EMBO Rep.* **3**, 975–981
19. Meehan, R. R., Kao, C. F., and Pennings, S. (2003) HP1 binding to native chromatin *in vitro* is determined by the hinge region and not by the chromodomain. *EMBO J.* **22**, 3164–3174
20. Smothers, J. F., and Henikoff, S. (2001) The hinge and chromo shadow domain impart distinct targeting of HP1-like proteins. *Mol. Cell. Biol.* **21**, 2555–2569
21. Liu, C., Xi, W. Y., Shen, L. S., Tan, C. P., and Yu, H. (2009) Regulation of floral patterning by flowering time genes. *Dev. Cell* **16**, 711–722
22. Zhu, Y., Luo, X., Liu, X. X., Wu, W. J., Cui, X. F., He, Y. H., and Huang, J. R. (2020) Arabidopsis PEAPODs function with LIKE HETEROCHROMATIN PROTEIN1 to regulate lateral organ growth. *J. Integr. Plant Biol.* **62**, 812–831
23. Berry, S., Rosa, S., Howard, M., Buhler, M., and Dean, C. (2017) Disruption of an RNA-binding hinge region abolishes LHP1-mediated epigenetic repression. *Genes Dev.* **31**, 2115–2120
24. Jackson, J. P., Lindroth, A. M., Cao, X., and Jacobsen, S. E. (2002) Control of CpNpG DNA methylation by the KRYPTONITE histone H3 methyltransferase. *Nature* **416**, 556–560
25. Zemach, A., Li, Y., Ben-Meir, H., Oliva, M., Mosquna, A., Kiss, V., Avivi, Y., Ohad, N., and Grafi, G. (2006) Different domains control the localization and mobility of LIKE HETEROCHROMATIN PROTEIN1 in Arabidopsis nuclei. *Plant Cell* **18**, 133–145
26. Yu, Y., Dong, A. W., and Shen, W. H. (2004) Molecular characterization of the tobacco SET domain protein NtSET1 unravels its role in histone methylation, chromatin binding, and segregation. *Plant J.* **40**, 699–711
27. Zhang, X., Germann, S., Blus, B. J., Khorasanizadeh, S., Gaudin, V., and Jacobsen, S. E. (2007) The Arabidopsis LHP1 protein colocalizes with histone H3 Lys27 trimethylation. *Nat. Struct. Mol. Biol.* **14**, 869–871
28. Turck, F., Roudier, F., Farrona, S., Martin-Magniette, M. L., Guillaume, E., Buisine, N., Gagnot, S., Martienssen, R. A., Coupland, G., and Colot, V. (2007) Arabidopsis TFL2/LHP1 specifically associates with genes marked by trimethylation of histone H3 lysine 27. *PLoS Genet.* **3**, e86
29. Cao, R., Wang, L. J., Wang, H. B., Xia, L., Erdjument-Bromage, H., Tempst, P., Jones, R. S., and Zhang, Y. (2002) Role of histone H3 lysine 27 methylation in polycomb-group silencing. *Science* **298**, 1039–1043
30. Czermin, B., Melfi, R., McCabe, D., Seitz, V., Imhof, A., and Pirrotta, V. (2002) Drosophila enhancer of Zeste/ESC complexes have a histone H3 methyltransferase activity that marks chromosomal polycomb sites. *Cell* **111**, 185–196
31. Libault, M., Tessadori, F., Germann, S., Snijder, B., Fransz, P., and Gaudin, V. (2005) The Arabidopsis LHP1 protein is a component of euchromatin. *Planta* **222**, 910–925
32. Nakahigashi, K., Jasencakova, Z., Schubert, I., and Goto, K. (2005) The Arabidopsis HETEROCHROMATIN PROTEIN1 homolog (TERMINAL FLOWER2) silences genes within the euchromatic region but not genes positioned in heterochromatin. *Plant Cell Physiol.* **46**, 1747–1756
33. Minc, E., Allory, Y., Courvalin, J. C., and Buendia, B. (2001) Immunolocalization of HP1 proteins in metaphasic mammalian chromosomes. *Methods Cell Sci.* **23**, 171–174
34. Cheutin, T., McNairn, A. J., Jenuwein, T., Gilbert, D. M., Singh, P. B., and Misteli, T. (2003) Maintenance of stable heterochromatin domains by dynamic HP1 binding. *Science* **299**, 721–725
35. Cheutin, T., Gorski, S. A., May, K. M., Singh, P. B., and Misteli, T. (2004) *In vivo* dynamics of Swi6 in yeast: Evidence for a stochastic model of heterochromatin. *Mol. Cell. Biol.* **24**, 3157–3167
36. Festenstein, R., Pagakis, S. N., Hiragami, K., Lyon, D., Verreault, A., Sekkali, B., and Kioussis, D. (2003) Modulation of heterochromatin protein 1 dynamics in primary Mammalian cells. *Science* **299**, 719–721
37. Mylne, J. S., Barrett, L., Tessadori, F., Mesnage, S., Johnson, L., Bernatavichute, Y. V., Jacobsen, S. E., Fransz, P., and Dean, C. (2006) LHP1, the Arabidopsis homologue of HETEROCHROMATIN PROTEIN1, is required for epigenetic silencing of FLC. *Proc. Natl. Acad. Sci. U. S. A.* **103**, 5012–5017
38. Sung, S., He, Y., Eshoo, T. W., Tamada, Y., Johnson, L., Nakahigashi, K., Goto, K., Jacobsen, S. E., and Amasino, R. M. (2006) Epigenetic maintenance of the vernalized state in Arabidopsis thaliana requires LIKE HETEROCHROMATIN PROTEIN 1. *Nat. Genet.* **38**, 706–710
39. Li, Z. F., Li, B., Liu, J., Guo, Z. H., Liu, Y. H., Li, Y., Shen, W. H., Huang, Y., Huang, H., Zhang, Y. J., and Dong, A. W. (2016) Transcription factors AS1 and AS2 interact with LHP1 to repress KNOX genes in Arabidopsis. *J. Integr. Plant Biol.* **58**, 959–970
40. Xu, L., and Shen, W. H. (2008) Polycomb silencing of KNOX genes confines shoot stem cell niches in Arabidopsis. *Curr. Biol.* **18**, 1966–1971
41. Bratzel, F., Lopez-Torrejon, G., Koch, M., Del Pozo, J. C., and Calonje, M. (2010) Keeping cell identity in arabidopsis requires PRC1 RING-Finger homologs that catalyze H2A monoubiquitination. *Curr. Biol.* **20**, 1853–1859
42. Derkacheva, M., Steinbach, Y., Wildhaber, T., Mozgova, I., Mahrez, W., Nanni, P., Bischof, S., Gruissem, W., and Hennig, L. (2013) Arabidopsis MSI1 connects LHP1 to PRC2 complexes. *EMBO J.* **32**, 2073–2085
43. Wang, H., Liu, C. M., Cheng, J. F., Liu, J., Zhang, L., He, C. S., Shen, W. H., Jin, H., Xu, L., and Zhang, Y. J. (2016) Arabidopsis flower and embryo developmental genes are repressed in seedlings by different combinations of polycomb group proteins in association with distinct sets of cis-regulatory elements. *PLoS Genet.* **12**, e1005771
44. Veluchamy, A., Jegu, T., Ariel, F., Latrasse, D., Mariappan, K. G., Kim, S. K., Crespi, M., Hirt, H., Bergounioux, C., Raynaud, C., and Benhamed, M. (2016) LHP1 regulates H3K27me3 spreading and shapes the three-dimensional conformation of the Arabidopsis genome. *PLoS One* **11**, e0158936
45. Zhou, Y., Tergemina, E., Cui, H. T., Forderer, A., Hartwig, B., James, G. V., Schneeberger, K., and Turck, F. (2017) Ctf4-related protein recruits LHP1-PRC2 to maintain H3K27me3 levels in dividing cells in Arabidopsis thaliana. *Proc. Natl. Acad. Sci. U. S. A.* **114**, 4833–4838
46. Fischle, W., Wang, Y., Jacobs, S. A., Kim, Y., Allis, C. D., and Khorasanizadeh, S. (2003) Molecular basis for the discrimination of repressive methyl-lysine marks in histone H3 by Polycomb and HP1 chromodomains. *Genes Dev.* **17**, 1870–1881
47. Kaustov, L., Ouyang, H., Amaya, M., Lemak, A., Nady, N., Duan, S., Wasney, G. A., Li, Z., Vedadi, M., Schapira, M., Min, J., and Arrowsmith, C. H. (2011) Recognition and specificity determinants of the human cbx chromodomains. *J. Biol. Chem.* **286**, 521–529
48. Ball, L. J., Murzina, N. V., Broadhurst, R. W., Raine, A. R., Archer, S. J., Stott, F. J., Murzin, A. G., Singh, P. B., Domaille, P. J., and Laue, E. D. (1997) Structure of the chromatin binding (chromo) domain from mouse modifier protein 1. *EMBO J.* **16**, 2473–2481
49. Jacobs, S. A., and Khorasanizadeh, S. (2002) Structure of HP1 chromodomain bound to a lysine 9-methylated histone H3 tail. *Science* **295**, 2080–2083
50. Min, J., Zhang, Y., and Xu, R. (2003) Structural basis for specific binding of polycomb chromodomain to histone H3 methylated at Lys 27. *Genes Dev.* **17**, 1823–1828
51. Zhang, M., Yang, Y., Zhou, M., Dong, A., Yan, X., Loppnau, P., Min, J., and Liu, Y. (2021) Histone and DNA binding ability studies of the NSD

subfamily of PWWP domains. *Biochem. Biophys. Res. Commun.* **569**, 199–206
52. Adams-Cioaba, M. A., and Min, J. (2009) Structure and function of histone methylation binding proteins. *Biochem. Cell Biol.* **87**, 93–105
53. Liu, Y., Tempel, W., Zhang, Q., Liang, X., Loppnau, P., Qin, S., and Min, J. (2016) Family-wide characterization of histone binding abilities of human CW domain-containing proteins. *J. Biol. Chem.* **291**, 9000–9013
54. Qin, S., and Min, J. (2014) Structure and function of the nucleosome-binding PWWP domain. *Trends Biochem. Sci.* **39**, 536–547
55. Liu, Y., Liu, K., Qin, S., Xu, C., and Min, J. (2014) Epigenetic targets and drug discovery: Part 1: Histone methylation. *Pharmacol. Ther.* **143**, 275–294
56. Exner, V., Aichinger, E., Shu, H., Wildhaber, T., Alfarano, P., Caflisch, A., Gruissem, W., Kohler, C., and Hennig, L. (2009) The chromodomain of LIKE HETEROCHROMATIN PROTEIN 1 is essential for H3K27me3 binding and function during Arabidopsis development. *PLoS One* **4**, e5335
57. Liu, Y., and Min, J. (2016) Structure and function of histone methylation-binding proteins in plants. *Biochem. J.* **473**, 1663–1680
58. Dong, C., Liu, Y., Lyu, T. J., Beldar, S., Lamb, K. N., Tempel, W., Li, Y., Li, Z., James, L. I., Qin, S., Wang, Y., and Min, J. (2020) Structural basis for the binding selectivity of human CDY chromodomains. *Cell Chem. Biol.* **27**, 827–838.e7
59. Zhao, S., Cheng, L., Gao, Y., Zhang, B., Zheng, X., Wang, L., Li, P., Sun, Q., and Li, H. (2019) Plant HP1 protein ADCP1 links multivalent H3K9 methylation readout to heterochromatin formation. *Cell Res.* **29**, 54–66
60. Du, J., Zhong, X., Bernatavichute, Y. V., Stroud, H., Feng, S., Caro, E., Vashisht, A. A., Terragni, J., Chin, H. G., Tu, A., Hetzel, J., Wohlschlegel, J. A., Pradhan, S., Patel, D. J., and Jacobsen, S. E. (2012) Dual binding of chromomethylase domains to H3K9me2-containing nucleosomes directs DNA methylation in plants. *Cell* **151**, 167–180
61. Kabsch, W. (2010) Xds. *Acta Crystallogr. D Biol. Crystallogr.* **66**, 125–132
62. Evans, P. R., and Murshudov, G. N. (2013) How good are my data and what is the resolution? *Acta Crystallogr. D Biol. Crystallogr.* **69**, 1204–1214
63. Mccoy, A. J., Grosse-Kunstleve, R. W., Adams, P. D., Winn, M. D., Storoni, L. C., and Read, R. J. (2007) Phaser crystallographic software. *J. Appl. Crystallogr.* **40**, 658–674
64. Emsley, P., Lohkamp, B., Scott, W. G., and Cowtan, K. (2010) Features and development of Coot. *Acta Crystallogr. D Biol. Crystallogr.* **66**, 486–501
65. Murshudov, G. N., Skubak, P., Lebedev, A. A., Pannu, N. S., Steiner, R. A., Nicholls, R. A., Winn, M. D., Long, F., and Vagin, A. A. (2011) REFMAC5 for the refinement of macromolecular crystal structures. *Acta Crystallogr. D Biol. Crystallogr.* **67**, 355–367
66. Langer, G., Cohen, S. X., Lamzin, V. S., and Perrakis, A. (2008) Automated macromolecular model building for X-ray crystallography using ARP/wARP version 7. *Nat. Protoc.* **3**, 1171–1179
67. Adams, P. D., Afonine, P. V., Bunkoczi, G., Chen, V. B., Davis, I. W., Echols, N., Headd, J. J., Hung, L. W., Kapral, G. J., Grosse-Kunstleve, R. W., McCoy, A. J., Moriarty, N. W., Oeffner, R., Read, R. J., Richardson, D. C., *et al.* (2010) Phenix: A comprehensive Python-based system for macromolecular structure solution. *Acta Crystallogr. D Biol. Crystallogr.* **66**, 213–221
68. Bayly, C. I., Cieplak, P., Cornell, W., and Kollman, P. A. (1993) A well-behaved electrostatic potential based method using charge restraints for deriving atomic charges: The RESP model. *J. Phys. Chem.* **97**, 10269–10280